

Experimental Analysis of Pressure Fluctuations and Hydrodynamics on Circulating Fluidized Beds

¹B. Chakrapani, ¹V. Pandu Rangudu, ²Vijaykumar Reddy and ¹B. Durga Prasa

¹Oil Research and Training Center,

Jawaharlal Nehru Technological University, Anantapur, India

²Jawaharlal Nehru Technological University, Hyderabad, India

Abstract: The pressure fluctuations in a fluidized bed are a result of the actions of the bubbles. However, the bubbles may be influenced by the air supply system and by the pressure drop of the air distributor. These Interactions are treated for low as well as for high velocity beds by means of a simple model of the principal frequency of the pressure fluctuations. The model includes the interaction with the air supply system and describes qualitatively two important bubbling regimes: the single bubble regime, important for systems with low pressure drop air distributors and the exploding bubble regime for high velocity beds.

Key words: Fluidized beds, bubbles, pressure fluctuations, air distributors, air supply system

INTRODUCTION

The pressure fluctuations in a fluidized bed are related to the movements of the Bed and particularly to the bubbles. This subject has been thoroughly investigated in the past, but there are reasons to continue the exploration of pressure fluctuations. Firstly, during recent years computers and data collection equipment have made registration of pressure signals and evaluation of data a relatively simple task. Secondly, available analyses were dedicated to bubbling conditions at low fluidization velocities, but the present interest also covers Circulating Fluidized Beds (CFB). Pressure fluctuations in CFB have been studied to characterize the state of fluidization. As the amplitude of pressure fluctuation increases during a rise of velocity, the CFB may pass several fluidization regimes, such as slugging, turbulent and fast fluidization, the latter regime being archeries by rather smooth conditions without bubbles. It appears that the CFB studies mentioned were carried out in high aspect ratio (bed height to bed width ratio) risers. In contrast, studies carried out in low aspect ratio risers, such as combustors, observed a behaviour reminding of a bubbling bed also at high gas velocities "1, 2". Therefore, there is a reason to account for the fluidization behaviour under various conditions, including those of bubbling CFB, by means of pressure analysis. The purpose of the present study is to illustrate the fluidization behaviour as seen from bed pressure fluctuations and to study the interaction with the gas volume below the bed.

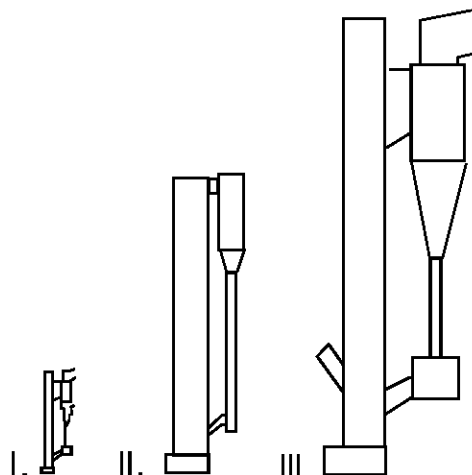


Fig. 1: The experimental equipment

Experimental conditions: Measurements were carried out in Three plants of different scale and design, Fig. 1. The absolute pressure was sampled from the dense bottom bed and from the air plenum below the air distributor. The properties of the three plants are listed in Table 1. Plant III is a 12 MW boiler described by Leckner *et al.* (1991). Plant I is a 1:9 cold scale model of the Boiler. Johnson *et al.* (1999) made a closer description of this plant and explained the scaling conditions. Plant II is a cold CFB laboratory rig with rectangular cross section. The size of the air supply system and particularly of the air plenum, can be

Table 1: Data of the research plants

Quantity	Plant 1	Plant 2	Plant
Cross section, A_{bed} [m ²]	0.16 · 0.19	0.12 · 0.70	1.47 · 1.42
Height of riser, [m]	1.5	8.5	13.5
Volume of air plenum, V_{ap} [m ³]	0.0028	0.45	2.04
Total volume of air supply system including pipes and air plenum, V [m ³]	0.0111	2.88	5.17
Air distributor	Perforated plate	Perforated plate	Bubble cap
Bed temperature, [°C]	40	40	40, 850
Fluidization velocity, U [m/s]	0.4-1.4	0.4-1.8	0.3-6.0
Bed material mean particle size, d	Iron	Silica sand	Silica sand
Particledensity, ρ_p [kg m ⁻³]	0.06	0.32	0.15-0.43
Height of dense bottom bed, H [m]	7860	2600	2600

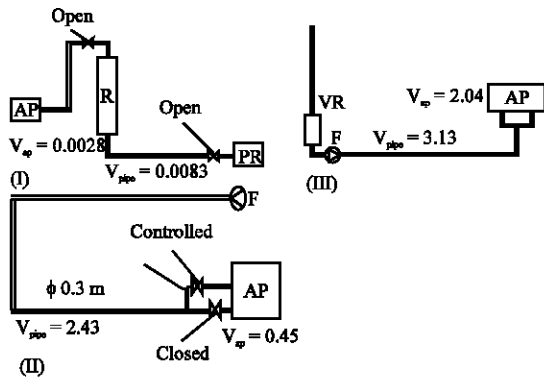


Fig. 2: Air feed systems (not scaled) in plants I, II and III. F_Fan, AP_Air Plenum, PR_Pressure Reducer of pressurized air system, R_Rotameter, VR_Velocity Reducing volume, V_{ap} _Volum of air plenum, [m³]. V_{pipe} _volume of air-feed pipes downstream of PR in I and F in II and III

important for the pressure fluctuations. Therefore, the air supply systems are shown roughly in Fig. 2.

Experimental results: The quality of fluidization was studied systematically in Plants II and III. As a result, Svensson *et al.* (1996) identified three fluidization regimes: Multiple bubble regime, single bubble regime and exploding bubble regime. In the multiple bubble regime numerous small bubbles are formed in the bed. This is reflected in the wide range of frequencies seen in the pressure spectrum. There is no correlation between the pressure fluctuation in the bed and in the air plenum. The distributor pressure drop is high. In the single bubble regime the bed is bubbling with large, regular bubbles, producing a narrow Frequency spectrum. This regime occurs at a combination of low pressure-drop distributor and low fluidization velocity. At high velocities bubbles become large. They look like irregular voids, whose size is limited by the height of the dense bottom bed. This is the exploding bubble regime.

Figure 3 shows an example of a gradual transition between the multiple bubble regime (a) and the single bubble regime (c) as the pressure drop across the distributor dp_{dist} is reduced at constant fluidization velocity $U = 0.4$ m/s. In these tests the ratio dp_{dist}/dp_{bed} ranged from 0.04 to above one, but the operation was deemed satisfactory in all cases, although the character of fluidization changed depending on the pressure drop. The dominant frequency of the wind box pressure was about 0.8 Hz in all tests shown in Fig. 3. Obviously, the connection between the wind box and the bed was small during operation with the high pressure-drop distributor (a), but in the case of the low pressure-drop distributor (c) there was a direct coupling between bed and wind box. At higher fluidization velocities in the same Plant II there was a direct connection between bed and wind box also at high pressure-drops and frequencies slightly higher than 1 Hz were observed. In this case the bubbles had an exploding character. In the boiler, the same bubble-cap distributor was used in all tests and the velocity was changed. This means that the pressure drop across the distributor also changed. The results are shown in Fig. 4, which illustrates a transition from single bubbling regime (a) to exploding bubbling regime (c) as the velocity increases. The intermediate case (b) in Fig. 4 is a transition case where the two regimes are present, as seen in the frequency domain. A similar occurrence of two regimes was previously shown in Fig. 3b. The advantage of operation under cold conditions and in a subsequent test under hot condition in the same unit (Svensson *et al.*, 1996) is that the results and the conclusions could be verified by independent optical fiber measurements. The transition was found also under hot (850°C) conditions, but it was not possible to operate as low as in the cold case (0.3 m/s), since the same gas flow is $(850 + 273)/(40 + 273)$ times as large in the bed under hot bed conditions. On the other hand, high velocities could be attained. Registrations were carried out.

The various regimes identified have not been explicitly mentioned in the early literature. Many researchers studying bed processes have probably aimed

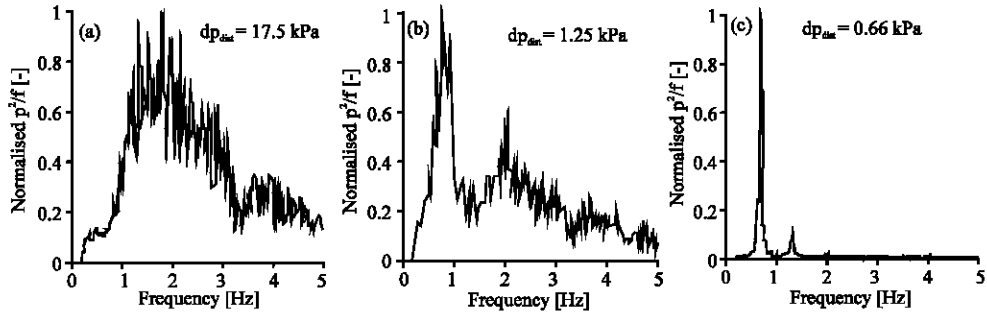


Fig. 3: In-bed pressure fluctuation spectra corresponding to a transition from multiple bubbling to single bubble regime in Plant II. $U = 0.4 \text{ m/s}$, $H = 0.6 \text{ m}$, $d = 0.32 \text{ mm}$ (Svensson *et al.*, 1996)

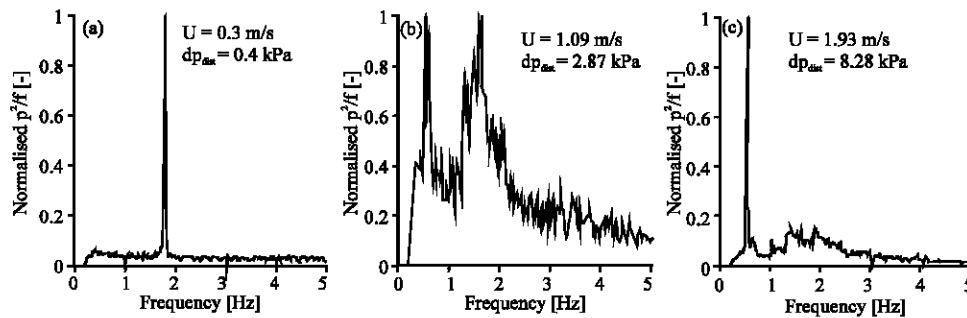


Fig. 4: Frequency spectra of pressure fluctuations in Plant III operated under cold conditions. $H = 0.3\text{-}0.4 \text{ m}$, $d = 0.15 \text{ mm}$ (Svensson *et al.*, 1996)

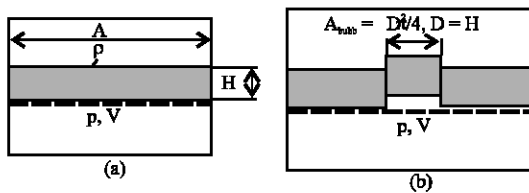


Fig. 5: Bubble models for (a) single and (b) exploding bubbles. Bed (grey) and air distributor (dashed)

at the high distributor pressure-drop case with multiple bubbles in order to achieve a well-behaved bubbling fluidized bed. However, also conditions similar to the single bubble regime have been observed and described, for instance by Baird and Klein (1973), Borodulya *et al.* (1985) and Baskakov *et al.* (1989). In the single bubble regime the bed behaves like a piston accelerated by a growing bubble, Fig. 5a. Davidson (1968) interpreted this behaviour as an interaction between the bed and the air plenum and derived an expression for the bubble frequency. Many researchers adopted Davidson's idea and also included the resistance of the distributor (Moritomi *et al.*, 1980) and the air supply system (Borodulya *et al.*, 1985). For the present purpose, it is sufficient to write the bubble frequency as:

$$f = 1/2\pi (vpA/PHV)^{1/2} \quad (1)$$

Mean pressure in the plenum, A bed (piston) surface area, ρ bed density, H bed height and V is the effective volume of the air supply system. The derivations were made for isothermal systems. In a combustor, the temperature is different in the bed and in the air plenum. Hence, a change of the gas density in the air plenum $\rho_{g,ap}$ is felt in the bed as a corresponding change in the gas density $\rho_{g,bed}$ at bed temperature. A derivation shows that the right hand side of Eq. 1 should be multiplied by a factor $(\rho_{g,bed}/\rho_{g,ap})^{1/2}$ to consider non-isothermal cases.

The principal difficulty in applying Eq. 1 lies in defining the effective gas Volume upstream of the air distributor. Does the volume of the wind box represent the Adequate volume V in Eq. 1 or is it necessary to include also parts of the ducts of the air supply system? Obviously the pressure pulses from the bed are felt in the entire air supply system in the case when no devices causing pressure drops are present (such as High-pressure air distributor, closed valves, meters etc.), Johnson *et al.* (1997). Here Fig. 2 and Table 1 both air plenum and the air supply system downstream of some valve could serve as effective air volume, V, but it is not

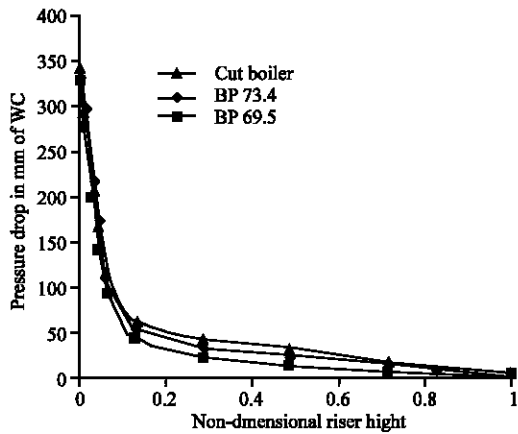


Fig. 6: Effect of particle size distribution

known how much of the air supply system that should be considered effective. Therefore, the results are shown below both with and without the air supply system. Another problem consists in defining the effective area of the piston. Above, A was taken to be the area of the bed, A_{bed} . However, for smaller bubbles one could imagine that only a vaguely defined part of the bed would move. In the case of an exploding bubble, the definition of an exploding bubble could be employed, Svensson *et al.* (1996), namely that the size of the Dubble (D) is limited by the height of the bed, $D \gg H$ and that the bubble opens up for a flow of gas that only lifts the part of the bed where the bubble acts, $A = A_{bubb} = pD^2/4$ in a three-dimensional bed. This case is illustrated in Fig. 5b. Once the plug of bed material is lifted, the gas escapes and the rest of the bed may not be affected.

Application: Agreement between the model, Eq. 1 and measured frequencies from single bubbles has been demonstrated by Baird and Klein (1973), Moritomi *et al.* (1980) and Bashkakov *et al.* (1989), but in view of the uncertainties mentioned, a further discussion is needed. A comparison between measurement data from the three plants and the model is shown in Fig. 6-8. The model is represented by two cases: the effective volume is either that of the air plenum or that of the plenum plus air supply system, as shown in Fig. 2 and Table 1. Figure 6 compares the frequencies obtained in the boiler with the model under both hot and cold conditions. The hot case has a hot bed and a cold air supply system (non-isothermal conditions), whereas in the cold case the bed and the air supply System have the same temperature (isothermal conditions). Qualitatively the results support the model approach: Indeed the difference between the single bubbles and explo fluidised ding bubbles is

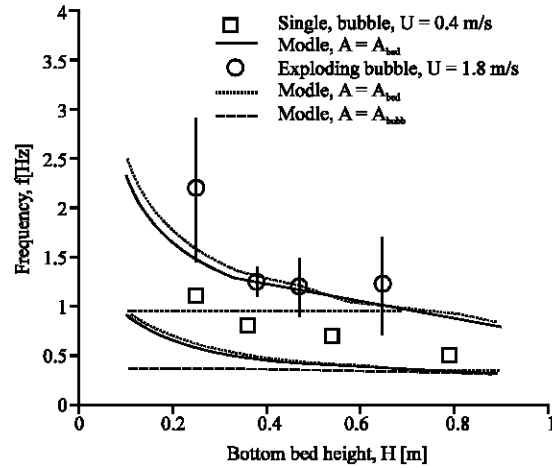


Fig. 7: Comparison between measured frequencies (symbols) from Plant II and model (curves). The thicker lines correspond

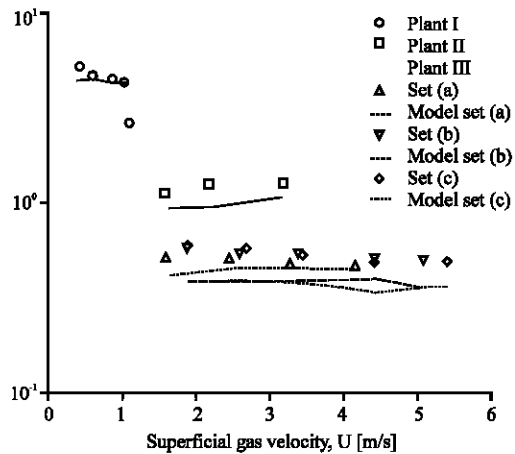


Fig. 8: Measured exploding bubble frequencies (symbols) in Plant I, II and III (hot) compared to model, $A = A_{bubb}$ (curves), dp_{ref} is reference pressure drop from 0.06-1.5 m above the air distributor. The lines represent $V = V_{sp}$.

described by the assumption of different active piston areas in Fig. 5. Within the range of uncertainties there is a systematic difference between single bubbles in the hot (Fig. 6a) and the cold (Fig. 6b) cases: The hot case coincides with $V = V_{ap}$ but the cold case with $V = V_t$. At present it is not possible to explain this difference, but a guess would be that the active areas are different for the high velocity (a) and the low velocity (b) cases of single bubbles, since they actually depend on bubble size, i. e. fluidization velocity. For example, agreement would be

obtained if the piston area were equal to half of the bed area in the low-velocity case and the area of the high-velocity.

The corresponding data from the cold rig, Plant II, are shown in Fig. 7. The agreement in Fig. 7 is qualitative, but within or close to the limits of uncertainty. The case of multiple bubbles was not in agreement and such data are not plotted (The reason is of course that in this case the bed is insulated from the air plenum by the high pressure-drop distributor).

In Fig. 8 exploding bubble frequencies from all three plants are compared. For clarity only the curves for $V = V_{ap}$ are drawn. The agreement is again qualitative, but reasonable, since $A = A_{bubb}$ used for modeling the exploding bubbles is an obvious approximation, considering the complex shape of the bubbles. The result is almost independent of velocity, which also agrees with the concept of exploding bubbles. It appears that the principal features of the fluctuations have been captured by the model, which is a severe task, bearing in mind the large differences in size and operation of the plants investigated.

HYDRO DYNAMICS OF FLUIDIZED BED

The 12 MWth CFB boiler has a cross-sectional area of 1.7 m by 1.5 m and a height of 13.4 m. The details are given Johnsson *et al.* (1999). Figure 9 shows the layout of the one-sixth scale-down model. The model was a geometrically similar riser, made of 10 mm thick acrylic sheet and the riser had a rectangular cross-section of dimensions 0.285×0.255 m and a height of 2.2 m. The cyclone separator was 0.180 m in diameter and 0.270 m in height and consisted of a tapered portion of length 0.450 m. The cyclone separator was connected to the riser through an exit duct of varying cross-section and slopes. The down comer had a butterfly valve to facilitate measurement of solid recycle flux and was connected to an L-valve through a storage box. The particles, which were collected in the vertical leg of the L-valve, were recycled to the riser with assist air from a compressor. A Pitot static tube located in the inlet pipeline measured the flow rate of the primary air supply. Ten pressure taps were located at distances, scaled down from the boiler, viz: 7, 22, 60, 85, 120, 245, 535, 902, 1320 and 1856 mm from the distributor plate. Axial pressure profiles in the riser were recorded with sand of particle size ($d_p = 125\ \mu\text{m}$), particle density ($2368\ \text{kg m}^{-3}$) and bed inventory of 24.2 kg and also with bronze of two particle size distributions (average $d_p = 69.5$ and $73.4\ \mu\text{m}$), particle density ($8563\ \text{kg m}^{-3}$) and bed inventory (24-28 kg). The fluidizing medium

was air at 35°C and 108 kPa. The fluidizing velocity range was 1.07-1.32 m/s. Sand was chosen to represent a commonly used bed material in laboratory investigations and bronze was the material that could be purchased to satisfy the scaling criteria as well as possible. The size distributions of the materials are shown in Fig. 10 compared with that of the boiler. $Ar = 110.7$, $Fr = 0.0554$ and $Re = 5.7$. The sphericity of particles is assumed to be unity for both boiler and the one-sixth model. Table 2-4 present the values of scaling and performance parameters (as deviations from the 12 MWth boiler data) for sand and bronze powder. Fluidizing velocity affects four of the nine parameters and is the most significant variable once the density ratio and bed inventory are fixed and, hence, data for four velocities are presented.

Scaling parameters: It is observed that the density ratio for bronze powder deviates from the CFB boiler value only by 12.8%, which is the best possible for laboratory experiments using readily available bought-out bed material. As expected, the deviation for sand was high, 76%. Froude number matching is best for $U = 1.08$ m/s for both bed materials; the deviation is only 2.5%. As the velocity increases, the deviation increases in all cases.

Fluidization Index matching is best for $U=1.32$ m/s and $d_p=73.4\ \mu\text{m}$ and the Archimedes number matches best for bronze of $73.4\ \mu\text{m}$ with the deviation of only 4%.

The Reynolds number matching was the best for bronze at $U = 1.25$ m/s ($d_p = 73.4\ \mu\text{m}$) and 1.32 m/s ($d_p = 69\ \mu\text{m}$). Of all the parameters, the no dimensional solid recycle flux, G^* , showed the worst matching for sand with deviation of 96%, while for bronze of $d_p = 69.5\ \mu\text{m}$ the deviation was 28%.

It is concluded from the above that operating with bronze, which has the lower deviation in density ratio is definitely acceptable. The question then is, which of the two sizes is better? From the U^* and Ar point of view, $73.4\ \mu\text{m}$ at 1.32 m/s is better. On the other hand, from the point of view of Re and G^* , bronze powder of $69.5\ \mu\text{m}$ at 1.32 m/s is acceptable. If Re and Ar matching is important, then $73.4\ \mu\text{m}$ is to be preferred. On the other hand, if Re and G^* matching is significant, then $69.5\ \mu\text{m}$ is to be recommended. If G^* matching is a must, bronze of $69.5\ \mu\text{m}$ at 1.32 m/s can be preferred if the deviation of 18% in Ar can be accepted.

From the above, it is clear that it is not possible to satisfy all scaling requirements for an atmospheric cold unit simultaneously. For the cold unit it is a choice between $73.4\ \mu\text{m}$ at 1.32 m/s or $69.5\ \mu\text{m}$ at 1.32 m/s. It can be concluded that PSD and fluidizing velocity play significant roles in matching.

Table 2: Sclaing parameters and performance parameters (Sand, 125 ¼m)

Fluidizing velocity, U m/s	1.08	1.17	1.25	1.32
Deviation in scaling parameters in %				
Geometry ratio (H*)	0	0	0	0
Froude no. (Fr)	-2.53	+14.4	+30.7	+45.7
Density ratio (Á*)	-75.9	-75.9	-75.9	-75.9
Fluidization index (U*)	+0.44	+8.8	+16.3	+22.8
Archimedes no. (Ar)	+29.4	+29.4	+29.4	+29.4
Reynolds no. (Re)	+45.5	+57.6	+68.4	+77.8
Non-dimensional solid recycle flux (Gs*)	-97.6	97.0	-96.7	-96.2
Per for mance parameters				
Riser pressure drop, mm WC 333 (boiler)	297	315	319	323
Deviation in pressure drop, %	-10.8	-5.4	-4.2	-3.0
RMS deviation for pressure profile, mm WC	±32.0	±40.3	±46.9	±50.6
Bottom bed height, % of non-dimensional riser height	5.5	5.3	5.2	5.1
Splash zone height, % of non-dimensional riser height	4.0 (boiler)	5.3-27.9	5.2-27.1	5.1-26.8
Transport zone height, % of non-dimensional riser height	5.5-28.2	27.9-100	27.1-100	26.8-100

Table 3: Scaling parameters and performance parameters (Bronze, 73.4 ¼m)

Fluidizing velocity, U m/s	1.08	1.17	1.25	1.32
Deviation in scaling parameters in %				
Geometry ratio (H*)	0	0	0	0
Froude no. (Fr)	-2.5	+14.4	+30.7	+45.7
Density ratio (Á*)	-12.8	-12.8	-12.8	-12.8
Fluidization index (U*)	-19.6	-9.9	-7.0	-1.8
Archimedes no. (Ar)	-4.0	-4.0	-4.0	-4.0
Reynolds no. (Re)	-14.2	-7.1	-0.72	+5.1
Non-dimensional solid recycle flux (Gs*)	-38.2	-37.9	-37.1	-36.8
Per for mance parameters				
Riser pressure drop, mm WC 333 (boiler)	324	331	351	364
Deviation in pressure drop,%	-2.7	-0.6	+5.4	+9.3
RMS deviation for pressure profile, mm WC	±26.5	±17.8	±9.8	±16.4
Bottom bed height, % of non-dimensional riser height	3.1	2.7	2.2	2.1
Splash zone height, % of non-dimensional riser height	4.0 (boiler)	2.7-21.12	2-19.7	2.1-17.1
Transport zone height, % of non-dimensional riser height	3.1-22.2	21.1-100	19.7-100	17.1-100

CFB Boiler Hydrodynamics

Table 4: Scaling parameters and performance parameters (Bronze, 69.5 ¼m)

Fluidizing velocity, U m/s	1.08	1.17	1.25	1.32
Deviation in scaling parameters in %				
Geometry ratio (H*)	0	0	0	0
Froude no. (Fr)	-2.5	+14.4	+30.7	+45.7
Density ratio (Á*)	-12.8	-12.8	-12.8	-12.8
Fluidization index (U*)	-10.7	-3.0	+3.7	+9.5
Archimedes no. (Ar)	-18.5	-18.5	-18.5	-18.5
Reynolds no. (Re)	-18.8	-12.0	-6.0	-0.74
Non-dimensional solid recycle flux (Gs*)	- 29.1	-28.8	-28.5	-28.0
Per for mance parameters				
Riser pressure drop, mm WC 333 (boiler)	321	339	347	360
Pressure drop deviation, boiler, %	- 36	+1.9	+4.2	+7.5
RMS deviation for pressure profile, mm WC	±17.0	±5.0	±12.0	±22.8
Bottom bed height, % of non-dimensional riser height	2.0	1.7	1.5	1.3
Splash zone height, % of non-dimensional riser height	2.5 (boiler)	1.7-19.9	1.47-20.1	1.3-21.2
Transport zone height, % of non-dimensional riser height	2.0-16.1	19.9-100	20.1-100	21.2-100

Performance parameters: Axial pressure profiles are presented in Fig. 3-7. Experiments with sand indicates the least matching of pressure profile (Fig. 3 and 7) with a RMS deviation in the range of ± 32 to 50 mm of water

column (Table 1), while for bronze it was ± 5 to 23 mm of water column with a lower value for 69.5¼ m at 1.17 m/s (Table 2 and 3, Fig. 4 and 5). In all cases the total riser pressure drop varies in the range of The bottom bed

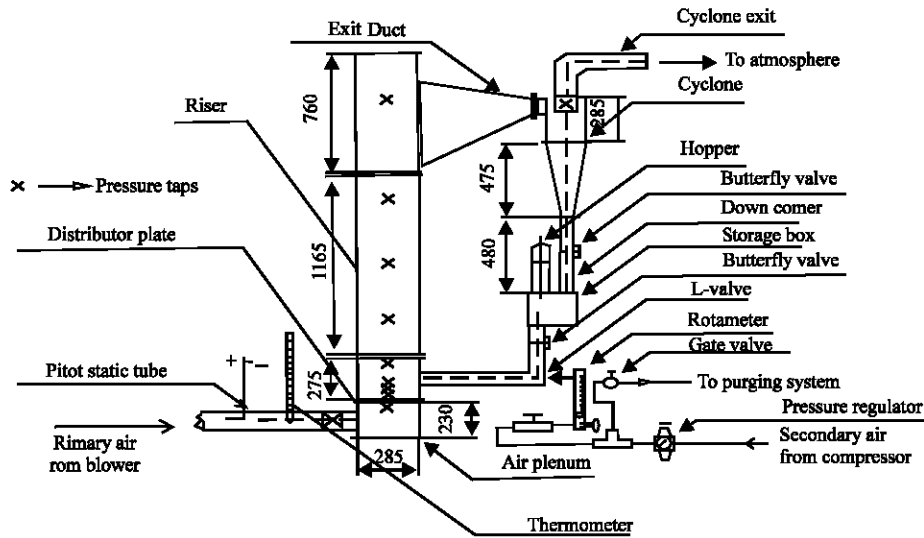


Fig. 9: The layout of the one-sixth scale-down model

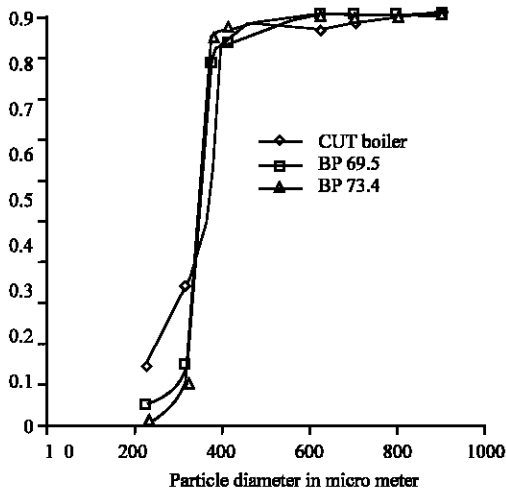


Fig. 10: Comparison of particle size distributions (Bronze 73.5 and 69.5 μm)

heights range from 5.1-5.5% of bed height for sand (as against 4.0% for the boiler) to 1.4- 2.0% of bed height for bronze of 69.5 μm (as against 2.5% for the boiler). As regards the transport zone, the 73.4 μm bronze at 1.17 m/s matched exactly with the boiler data, while 69.5 μm bronze matched exactly with boiler values at 1.32 m/s. For sand all the bottom bed heights are under-predicted.

The two bronze size distributions were quite close to each other and they both deviated from the size distribution of the boiler's bed material, as seen by the superimposed curves in Fig. 2. However, the matching of

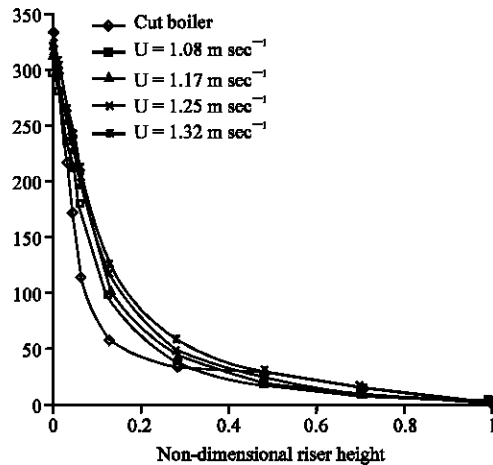


Fig. 11: Effect of fluidizing velocity (Sand 125 μm)

the pressure distributions is reasonable both bronze powders, Fig. 6, whereas there is a distinct difference in the sand case. Figure 7 0.6-10%, with bronze showing more acceptable deviation for the entire velocity range, the lowest being a 0.6% deviation for 73.4 μm at 1.17 m/s velocity.

The bottom bed heights range from 5.1-5.5% of bed height for sand (as against 4.0% for the boiler) to 1.4- 2.0% of bed height for bronze of 69.5 μm (as against 2.5% for the boiler). As regards the transport zone, the 73.4 μm bronze at 1.17 m/s matched exactly with the boiler data, while 69.5 μm bronze matched exactly with boiler values at 1.32 m/s. For sand all the bottom bed heights are under-predicted (Fig. 11-13).

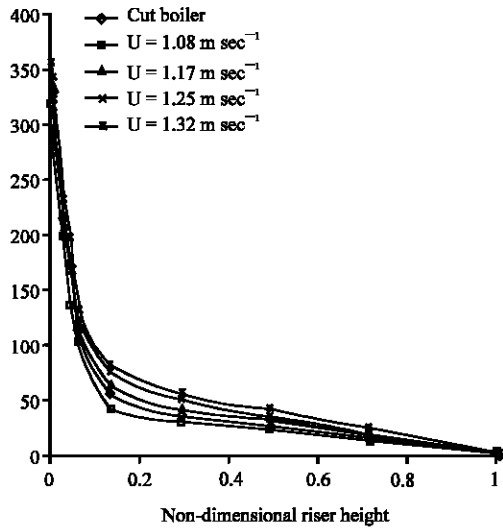


Fig. 12: Effect of fluidizing velocity (Bronze 69.5 μm)

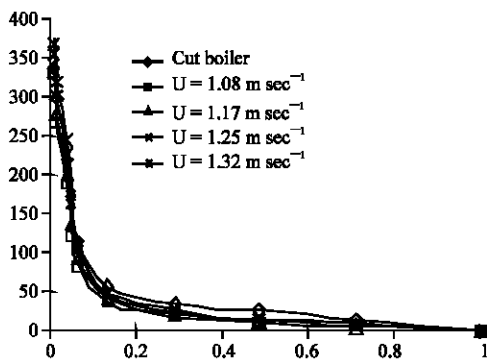


Fig. 13: Effect of fluidizing velocity (Bronze 73.4 μm)

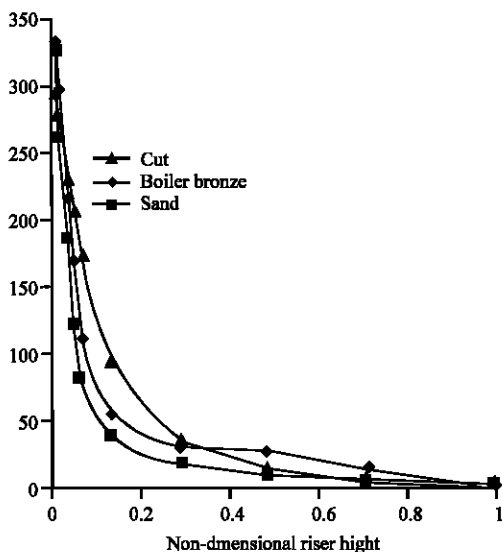


Fig. 14: Effect of density ratio

The two bronze size distributions were quite close to each other and they both deviated from the size distribution of the boiler's bed material, as seen by the superimposed curves in Fig. 10. However, the matching of the pressure distributions is reasonable both bronze powders, Fig. 14, whereas there is a distinct difference in the sand case.

CONCLUSION

In a previous research three bubbling modes were defined: multiple bubble regime (low velocities, high distributor pressure drop), single bubble regime (low distributor pressure drop) and exploding bubble regime (high velocity). The bottom bed of a CFB boiler produces exploding bubbles that appear like outburst of bed material from the bottom bed. These bubbles are limited in size by the height of the bottom bed and result in a considerable through-flow of gas (In fact, this is the explanation to why the bed can be maintained in the bottom of the CFB despite the high fluidization velocity). There is a gradual transition between regimes and under transition conditions they may occur intermittently during a certain period of observation. Because of the high pressure-drop across the air distributor required for a multiple bubble regime such a regime will not occur in a CFB combustor.

The frequency model describes qualitatively the measured frequencies in the Three very different beds investigated. There are two principal reasons for the Uncertainty of interpretation: the size of the active volume in a system with air supply ducts and the size of the active area of the bed (the piston). In the exploding bubble case the definition of an exploding bubble can be used to determine the piston area, an approach that agrees with measurements. This gives an indication of the qualitative correctness of the model concept.

Further research is necessary to interpret the variations of the fluctuations, especially the interactions between bed and air supply system, not only in order to learn more about the determination of the effective volume, that caused a considerable uncertainty in the present estimates, but also to understand the impact of fluid transients in the long pipes of the air supply systems. These transients may have a considerable influence on the fluidization behaviour, but they were not considered in the present research.

REFERENCES

Andersson, S., F. Johnsson and B. Leckner, 1989. Fluidization Regimes in Non-Slugging Fluidized Beds, Proceedings (A.M. Manaker) (Ed.). 10th International FBC Conference, San Francisco, ASME., 1: 239-247.

- Baird, M.H. and A.L. Klein, 1973. Spontaneous Oscillation of a Gas-Fluidized Bed. *Chem. Eng. Sci.*, pp: 28.
- Borodulya, V.A., V.V. Zavyalov and A. Buyevich Yu, 1985. Fluidized Bed Self-Oscillations. *Chem. Eng. Sci.*, 40: 353-364.
- Baskakov, A.P., N.F. Fillipovski and A.B. Mydrechenko, 1989. Influence of the Volume of the Sub-Distributor Chamber and Resistance of the Distributor on the Character of Fluidisation (in Russian), *Izvestia Vuzov, Belaruskij Politekhnikeskij Institute*, N1.
- Davidson, J.F., 1968. First Session_Introduction by Rapporteur. *I. Chem. E. Symp. Series*, 30: 3-11.
- Svensson, A., F. Johnsson and B. Leckner, 1996. Bottom Bed Regimes in a Circulating Fluidized Bed Boiler. *Int. J. Multiphase Flow*, 22: 1187-1204.
- Johnsson, F., R.C. Zijerveld and B. Leckner, 1997. Air-Plenum Pressure Fluctuations in a Circulating Fluidized Bed Boiler. *Proceedings (M. Olazar, M.J. San José) (Eds.). 2nd European Conference on Fluidization, Bilbao, Spain*, pp: 223-230.
- Johnsson, F., A. Vragar and B. Leckner, 1999. Solids Flow Pattern in the Exit Region of a CFF Furnace_Influence of Exit Geometry. *Proceedings (R.B. Reuther) (Ed.). 15th International FBC Conference, Savannah, USA, ASME.*, 1: 164-184.
- Leckner, B., M. Golriz, W. Zhang, B.Å. Andersson and F. Johnsson, 1991. Boundary Layers_First Measurements in a 12 MW CFB Research Plant at Chalmers University. *Proceedings (E.J. Anthony) (Ed.). 11th International FBC Conference, Montreal, Canada, ASME.*, 2: 771-776.
- Moritomi, H., S. Mori, K. Araki and A. Moriyama, 1980. Periodic Pressure Fluctuation in a Gaseous Fluidized Bed. *Kagaku Kogaku Ronbunshu*, 6: 392-396.
- Svensson, A., F. Johnsson and B. Leckner, 1996. Fluidization Regimes in Non-Slugging Fluidized Beds: The Influence of Pressure Drop Across the Air Distributor, *Powder Tech.*, 86: 299-312.